Checkpoint proteins control morphogenetic events during DNA replication stress in *Saccharomyces cerevisiae*

Jorrit M. Enserink,[1] Marcus B. Smolka,[1] Huilin Zhou,[1,3,4] and Richard D. Kolodner[1,2,3,4]

[1]Ludwig Institute for Cancer Research, [2]Department of Medicine, [3]Department of Cellular and Molecular Medicine, and [4]Cancer Center, University of California, San Diego School of Medicine, La Jolla, CA 92093

In response to DNA replication stress in *Saccharomyces cerevisiae*, the DNA replication checkpoint maintains replication fork stability, prevents precocious chromosome segregation, and causes cells to arrest as large-budded cells. The checkpoint kinases Mec1 and Rad53 act in this checkpoint. Treatment of *mec1* or *rad53Δ* mutants with replication inhibitors results in replication fork collapse and inappropriate partitioning of partially replicated chromosomes, leading to cell death. We describe a previously unappreciated function of various replication stress checkpoint proteins, including Rad53, in the control of cell morphology. Checkpoint mutants have aberrant cell morphology and cell walls, and show defective bud site selection. Rad53 shows genetic interactions with septin ring pathway components, and, along with other checkpoint proteins, controls the timely degradation of Swe1 during replication stress, thereby facilitating proper bud growth. Thus, checkpoint proteins play an important role in coordinating morphogenetic events with DNA replication during replication stress.

Introduction

Tight coordination of the cellular events associated with every phase of the cell cycle is essential for orderly progression through the cell cycle (Hartwell and Weinert, 1989). Cells arrest the cell cycle when confronted with stresses that may compromise cellular integrity. The mechanisms that halt the cell cycle are referred to as checkpoints (Hartwell and Weinert, 1989). Checkpoints result in key dependency relationships; mutants that fail to complete DNA replication also block nuclear division and cytokinesis, and mutants that fail to complete nuclear division also block cytokinesis (Hartwell and Weinert, 1989). Cells arrest the cell cycle in response to DNA damage. The DNA damage checkpoint was originally defined as the pathway that promotes cell cycle delay in response to DNA damage (Hartwell and Weinert, 1989), although it is now generally accepted that checkpoint responses involve additional processes, such as the activation and recruitment of DNA repair factors (Lisby et al., 2004) and the stabilization of replication forks (Lopes et al., 2001). At least two checkpoints operate during S phase in *Saccharomyces cerevisiae*; the replication checkpoint, which was originally defined as causing hydroxyurea (HU)-induced cell cycle arrest and inhibition of late-firing origins (Santocanale and Diffley, 1998), and the intra–S phase checkpoint, which reduces the rate of DNA replication and slows cell cycle progression in response to DNA-damaging agents (Paulovich et al., 1997). A series of checkpoints also act to monitor assembly of the mitotic spindle and regulate progression through mitosis (Kops et al., 2005). More recently, additional checkpoints have been identified, including a cell wall morphology checkpoint and a morphogenesis checkpoint, which monitor cell wall synthesis, bud formation, cell size, actin perturbation and, possibly, septin organization (Kellogg, 2003; Lew, 2003; Suzuki et al., 2004).

DNA replication stress and DNA damage induce activation of two phosphoinositide 3-kinase–related kinases, Tel1 and Mec1, which are similar to mammalian ataxia telangiectasia mutated and ataxia telangiectasia mutated and Rad3-related. These function in the activation of downstream protein kinases, including Chk1 and Rad53. Activation of Rad53 (*S. cerevisiae* Chk2) is mediated by two partially redundant adaptor proteins Mrc1 and Rad9 (Alcasabas et al., 2001). Although in *Schizosaccharomyces pombe* and higher eukaryotes cell cycle progression is blocked in response to replication stress, mainly by stimulating inhibitory phosphorylation of cyclin-dependent kinases (CDKs), in *S. cerevisiae* inhibition of Cdk1 (*S. cerevisiae* CDK) activity does not appear to play a role in S phase

Correspondence to Richard D. Kolodner: rkolodner@ucsd.edu

Abbreviations used in this paper: CDK, cyclin-dependent kinase; HU, hydroxyurea; YPD, yeast extract/peptone/dextrose.

The online version of this article contains supplemental material.

The Journal of Cell Biology, Vol. 175, No. 5, December 4, 2006 729–741
http://www.jcb.org/cgi/doi/10.1083/jcb.200605080

checkpoint-induced cell cycle arrest (Amon et al., 1992; Sorger and Murray, 1992). Rather, *S. cerevisiae* blocks cell cycle progression by directly inhibiting late origin firing and chromosome segregation (Santocanale and Diffley, 1998; Sanchez et al., 1999). Cdk1 in *S. cerevisiae* appears to have taken on a different function, and it synchronizes bud morphogenesis with the cell cycle (Lew, 2003). In *S. cerevisiae*, Cdk1 activity is determined by various factors, including Swe1 (*S. cerevisiae* equivalent of mammalian and *S. pombe* Wee1), which phosphorylates the conserved Y19 residue on Cdk1, resulting in inhibition of Cdk1. This phosphorylation is removed by the phosphatase Mih1. Swe1 levels are controlled by a pathway often referred to as the morphogenesis checkpoint (Lew, 2003), which responds to the state of the actin cytoskeleton, bud formation, and cell size, resulting in accumulation of Swe1, thereby delaying entry into mitosis (Kellogg, 2003; Lew, 2003). Degradation of Swe1 depends on various factors, including septins. Septins serve as a scaffold to recruit Swe1 and various kinases that phosphorylate Swe1, ultimately targeting it for destruction by an as yet unknown Skp1–Cul1–F-box complex and, possibly, the anaphase-promoting complex (McMillan et al., 2002; Thornton and Toczyski, 2003). A defect in Swe1 degradation results in prolonged inhibition of Cdk1. As a consequence, Cdk1 cannot induce the switch from polar to isotropic bud growth, resulting in the formation of elongated buds (Pruyne and Bretscher, 2000a,b).

Thus far, studies on the S-phase checkpoints have mainly focused on regulation of DNA replication, replication fork stabilization, and chromosome segregation. We show a novel role for components of the replication stress checkpoints in control of morphogenesis during replication stress. Our results are consistent with a model in which checkpoint proteins promote timely degradation of Swe1, thereby restricting bud growth during replication stress.

Results

Checkpoint-defective mutants have aberrant cell morphology

We observed that checkpoint mutants frequently have morphological aberrations. For instance, *mec1 tel1* double mutant cells are commonly misshapen, have somewhat elongated buds, and often fail to complete cytokinesis (Fig. 1 A). *rad9* and *mrc1Δ* single mutants did not have morphological aberrations (unpublished data), whereas mutants lacking both Mrc1 and Rad9, which function upstream of Rad53 (Alcasabas et al., 2001), as well as *rad53Δ* mutants had a phenotype similar to that of *mec1 tel1* mutants (Fig. 1 A). Deletion of *DUN1*, which acts downstream of Rad53, resulted in a milder phenotype, whereas *mec1* and *chk1* mutants did not have a morphology defect (unpublished data). In addition, *mec1 tel1* and *mrc1Δ rad9* double mutants, and *rad53Δ* single mutants, frequently deposited abnormally large amounts of chitin (Fig. 1 A), not only at the bud neck but often at other apparently random sites of the cell wall (unpublished data), suggesting a possible defect in orchestrating cell wall architecture. Because cells with defective cell walls lyse in the presence of SDS or Calcofluor white (Lussier et al., 1997; Bickle et al., 1998), we tested the sensitivity of various mutants to these chemicals. *mec1*, *tel1*, and *chk1* single mutants were no more sensitive to Calcofluor white and SDS than wild-type cells, whereas *rad53Δ* mutants were one to two orders of magnitude more sensitive (Fig. 1 B), which is indicative of a defective cell wall architecture. *mec1 tel1* double mutants showed severely reduced viability on yeast extract/peptone/dextrose (YPD), probably because these cells suffer major endogenous DNA damage from lack of DNA repair and checkpoint functions (Myung et al., 2001), and these mutants were sensitive to Calcofluor white (Fig. S1 A, available at http://www.jcb.org/cgi/content/full/jcb.200605080/DC1). However, because of the dramatic growth defects of *mec1 tel1* double mutants, we decided to focus on *rad53Δ* and *mrc1Δ rad9* mutants instead. *mrc1Δ rad9* mutants were as sensitive to Calcofluor white as *rad53Δ* mutants (Fig. S1 A), whereas *dun1* and *chk1* mutants were only weakly sensitive to Calcofluor white (Fig. S1 A). Therefore, Rad53 seems to be a critical mediator of resistance to Calcofluor white, whereas there appear to be redundancies between Mec1 and Tel1, between Rad9 and Mrc1, and, potentially, between Chk1 and Dun1 (not tested), paralleling the roles of these proteins in checkpoints (Cobb et al., 2004). Cells with cell wall defects are usually more sensitive to zymolase (Ovalle et al., 1998). Untreated wild-type and *rad53Δ* mutants did not lyse when incubated with a hypotonic buffer containing zymolase (Fig. 1 C). However, pretreatment with HU increased sensitivity of *rad53Δ* mutants to zymolase, whereas wild-type cells remained unaffected. Cell lysis typically occurred at the bud tips (unpublished data), indicating that the replication checkpoint promotes formation of a healthy bud during replication stress (see below). Cell wall stress activates the Pkc1–Slt2 pathway (Cid et al., 1995), and, consistent with our findings that checkpoint mutants have cell wall defects, Slt2 is hyperphosphorylated in *mec1 tel1* and *rad53Δ* mutants (Fig. 1 D). These results suggest that *mec1 tel1* and *mrc1Δ rad9* double mutants, and *rad53Δ* single mutants, have considerable defects in control of cell morphology and cell wall structure. Finally, we noticed that in *rad53Δ* mutants bud scars are frequently positioned at distal poles or at random positions on the cell (Fig. 1 E), indicating that *rad53Δ* mutants may have a bud site–selection defect because wild-type haploid cells have an axial budding pattern, forming buds at just one pole (Fig. 1 E; Pruyne and Bretscher, 2000a). As shown in Fig. 1 F, the majority of wild-type cells had an axial budding pattern. However, ∼45% of log phase *rad53Δ* mutants had bud scars that deviated from that pole. Cells expressing a kinase-dead mutant of *RAD53* (*rad53-KD*; K227A, D319A, and D339A; see Smolka et al. on p. 743 of this issue), which results in a checkpoint deficiency similar to that of *rad53Δ* mutants, had a bud site selection defect similar to that of a *rad53Δ* mutant (Fig. 1 F), indicating that the kinase function of Rad53 is essential for correct bud site selection. Furthermore, whereas *chk1*, *mec1*, and *tel1* mutants had very mild or no bud site selection defects, *mec1 tel1* double mutants had a bud site selection defect similar to that of *rad53Δ* mutants, whereas *rad9* and *dun1* mutants had a more intermediate phenotype. *bud1* mutants were examined as a control and were found to have a 100% random distribution of bud scars (unpublished data).

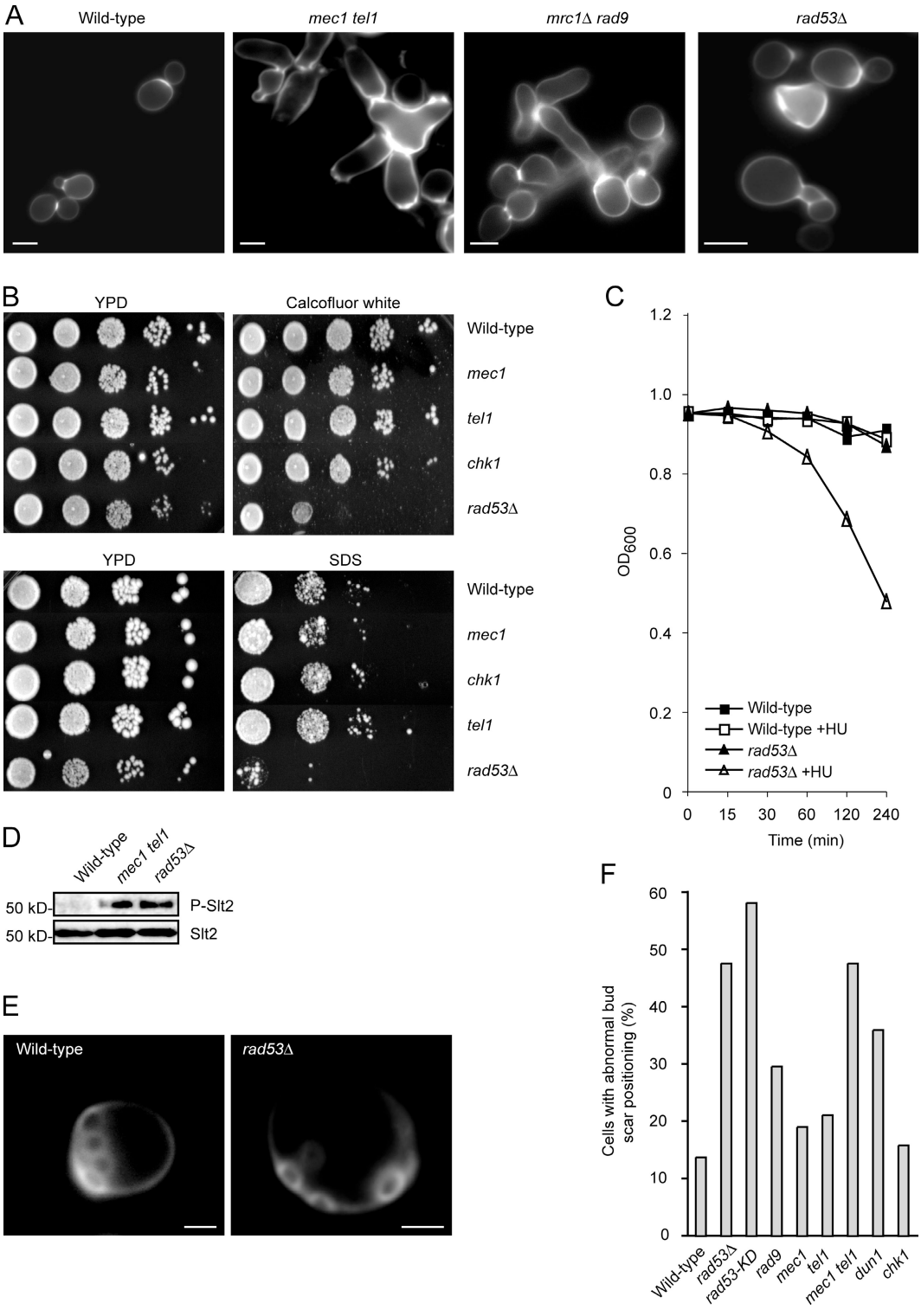

Figure 1. **Analysis of morphological aberrations in S-phase mutants.** (A) Aberrant morphology of checkpoint-defective mutants. Cell walls were visualized with Calcofluor white. (B) Cell wall defect in *rad53Δ* mutants. 10-fold dilutions of cultures were spotted on YPD plates and on 50 μg/ml Calcofluor white or 0.01% SDS. (C) *rad53Δ* mutants lyse when treated with zymolase. Cells were left untreated or treated with 200 mM HU for 4 h, after which a zymolase sensitivity assay was performed. (D) Hyperphosphorylation of Slt2 in checkpoint mutants. Cell lysates of log-phase cells were analyzed for phosphorylated Slt2. Equal sample loading was confirmed using pan-Slt2 antibodies. (E) Example of random budding patterns in *rad53Δ* mutants. Log-phase cells were stained with Calcofluor white to visualize bud scars. (F) Quantification of random budding patterns in various checkpoint mutants. Log-phase cells were stained with Calcofluor white to visualize the bud scars, and at least 100 cells with three or more bud scars were scored per strain. S288c strains were used. Bars: (A) 5 μm; (E) 1 μm.

In conclusion, we found that various checkpoint proteins contribute to cell wall architecture and maintenance of cell polarity.

Checkpoint proteins regulate the actin cytoskeleton during replication stress

Both bud site selection and cell wall synthesis are controlled by factors that regulate the actin cytoskeleton (Pruyne and Bretscher, 2000a). To test whether S-phase checkpoint proteins function in regulation of the actin cytoskeleton, we treated log-phase wild-type cells with HU for 4 h and visualized F-actin using rhodamine-phalloidin. Untreated wild-type, *chk1*, *rad53Δ*, and *mrc1Δ rad9* mutants had a polarized actin cytoskeleton, with actin cables extending from the mother cell into the bud (Fig. 2, A and B). Treatment of wild-type cells with HU arrested the cells with large buds and a depolarized actin cytoskeleton (Fig. 2, A and B). In contrast, the actin cytoskeleton of both *rad53Δ* and *mrc1Δ rad9* mutant cells remained polarized upon HU treatment (Fig. 2, A and B). Incubation of *rad53Δ* mutants at 42°C for 5 min resulted in complete actin depolarization, showing that *rad53Δ* mutants did not have a general defect in stress responses (unpublished data). HU also failed to induce actin depolarization in *rad53-KD* mutants. *dun1* mutants, as well as *sgs1* mutants (a DNA helicase that is thought to play roles in both the replication and intra–S phase checkpoints; Frei and Gasser, 2000), also failed to fully depolarize the actin cytoskeleton. *tel1* and *chk1* mutants were similar to wild-type cells, and in *mec1* mutants, HU treatment only partially depolarized the actin cytoskeleton (Fig. 2 B, Fig. S1 B, and not depicted). Together, these results suggest that checkpoint proteins like Sgs1, Dun1, Rad53, and a combination of Mrc1 and Rad9 affect the polarity state of the actin cytoskeleton upon induction of replication stress.

Cytoskeletal polarity is guided by the Cdc24–Cdc42 pathway (Pruyne and Bretscher, 2000a). We found that in wild-type cells, treatment with HU resulted in the disappearance of Cdc24 from the bud tip membrane (Fig. 2 C), as might be expected from cells that have arrested with large buds. However, in *rad53Δ* and *dun1* single mutants, and in *mrc1Δ rad9* double mutants, Cdc24 remained at the membrane (Fig. 2 D), whereas *chk1* mutants were similar to wild-type cells. Similar results were obtained with cells expressing Sec4-GFP, a Rab GTPase that is an essential component of the secretory machinery found primarily at sites of polarized growth (Guo et al., 1999; Fig. S1 C). Therefore, these results indicate that checkpoint proteins, including Rad53, Dun1, and Mrc1, in combination with Rad9, promote removal of the bud growth machinery from the bud tip upon treatment with HU.

Mutations in genes involved in regulation of the actin cytoskeleton often render cells sensitive to pharmacological actin inhibitors like latrunculin A (Ayscough et al., 1997). Therefore, we speculated that *rad53Δ* mutants might also be sensitive to latrunculin A. As shown in Fig. 2 E, *rad53Δ* mutants were more sensitive to latrunculin A than wild-type cells, whereas *mec1*, *tel1, chk1*, and *dun1* single mutants were no more sensitive to latrunculin A than wild-type cells (Fig. 2 E and not depicted). Interestingly, a *swe1* deletion suppressed the sensitivity of *rad53Δ* mutants to latrunculin A (Fig. 2 E), and we found that Rad53 may control Swe1 (see the following section).

Swe1-dependent control of bud growth by checkpoint proteins during replication stress

In addition to failure to depolarize the actin cytoskeleton, treatment of *rad53Δ*, but not wild-type, cells with HU for extended periods of time (16–20 h, although visible after 6 h [see Smolka et al. on p. 743 of this issue], after which >80% of the cells are still alive, as indicated by staining with vital dyes; Fig. S2 A, available at http://www.jcb.org/cgi/content/full/jcb.200605080/DC1) resulted in formation of elongated buds (Fig. 3, A and C). Analysis of W303 *RAD5* and W303 *RAD5 rad53Δ sml1* strains revealed a similar effect of a *rad53Δ* mutation (unpublished data). Formation of elongated buds is a common feature of mutants that fail to properly control levels of Swe1 (Pruyne and Bretscher, 2000b). This, and the finding that deletion of *SWE1* suppressed the sensitivity of *rad53Δ* mutants to latrunculin A, raised the possibility that the elongated bud phenotype of HU-treated *rad53Δ* mutants is caused by failure to down-regulate Swe1. Indeed, deletion of *SWE1* completely rescued the HU-induced elongated bud phenotype of the *rad53Δ* mutant (Fig. 3, B and C). Similar results were obtained with cells harboring the *rad53-KD* allele (Fig. 3 C and Fig. S2 B). Deletion of *DUN1* also caused cells to form elongated buds after treatment with HU (Fig. 3 C), and deletion of *DUN1* in a *rad53Δ* background resulted in an augmented phenotype (Fig. 3 C).

We next tested the effect of a range of mutations in genes encoding checkpoint functions on bud morphogenesis during replication stress. *rfc5-1*, *tel1*, *mec1*, *mrc1Δ*, and *rad9* single mutations all caused no, or a very small, increase in HU-induced elongated bud growth. In contrast, *rad9 mrc1Δ* and *rad9 mrc1-AQ* double mutants, the latter of which express an allele of Mrc1 that is proficient in DNA replication, but unable to activate the replication checkpoint (Osborn and Elledge, 2003), showed elongated bud growth upon HU treatment. Furthermore, *mec1 tel1* double mutants also showed an increase in elongated bud growth; however, we noticed that cells that attempted to elongate their buds frequently lysed, possibly because of their severe cell growth and cell wall defects, and this may obscure the phenotype. The *dpb11-1*, *tof1*, *csm3*, *chk1*, *rad17*, and *rad24* mutations alone did not increase HU-induced elongated bud growth (Fig. 3 C). In contrast, cells harboring the *rfa1-t11* allele displayed considerable HU-induced bud elongation, which is consistent with the function of the replication protein A complex in the DNA replication stress response. *sgs1* mutants also showed HU-induced elongated bud growth, which was *SWE1*-dependent, and the extent of elongation of these buds was often severe (Fig. S2 B). The *sgs1 rad24* double mutant had a more severe HU-induced elongated bud phenotype compared with the respective single mutants, similar to a previous report on the effects of *sgs1* and *rad24* mutations on the sensitivity to HU (Frei and Gasser, 2000). Other combinations of mutations did not reveal significant genetic interactions (Fig. 3 C). Finally, mutations in *MRE11*, *RAD50*, and *XRS2*, which are the three components of the MRX complex, resulted in HU-induced

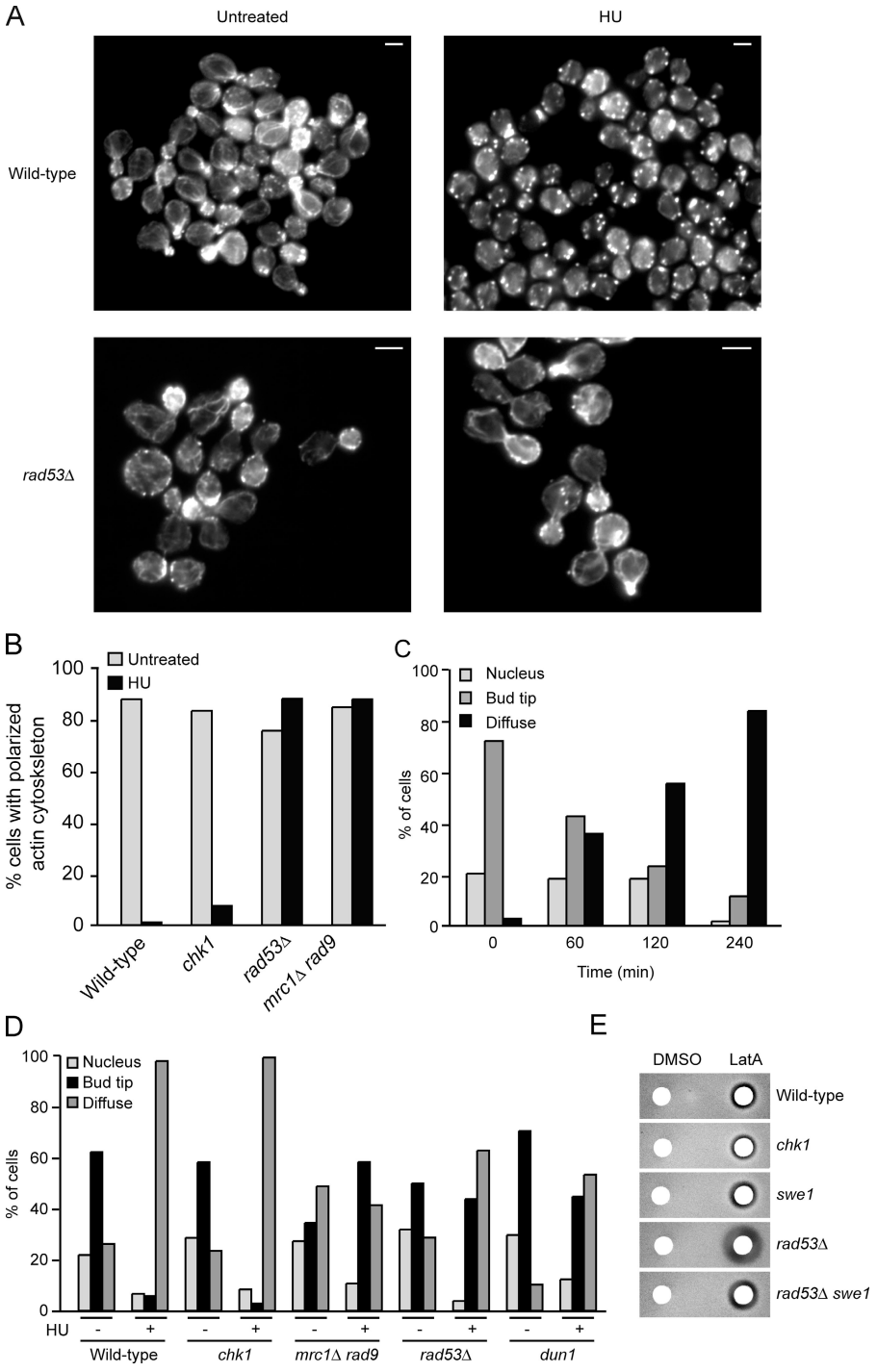

Figure 2. **Regulation of the actin cytoskeleton during replication stress.** (A) Treatment with HU results in actin depolarization. Cells were treated with 200 mM HU for 3 h before being fixed and stained with rhodamine-phalloidin. Bars, 5 μm. (B) Quantification of cells with a polarized actin cytoskeleton. Cells were treated as in A, and at least 100 cells per treatment were counted. (C) Cdc24 is removed from bud tips upon HU treatment. Wild-type cells expressing Cdc24-GFP were treated with 200 mM HU for the indicated times, and localization of Cdc24 in budded cells was determined by fluorescence microscopy. (D) Cdc24 is not removed from bud tips upon HU treatment in replication checkpoint mutants. Log-phase cultures were left untreated or treated for 4 h with 200 mM HU, and localization of Cdc24 in only budded cells was determined as in C. (E) *rad53Δ* mutants are sensitive to latrunculin A in a Swe1-dependent manner. Halo assays were performed using 200 μM latrunculin A (LatA) or DMSO as a control. S288c strains were used.

elongated bud growth. These results identify Sgs1, the MRX complex, replication protein A, Mec1 in combination with Tel1, Mrc1 in combination with Rad9, Rad53, and Dun1 as important mediators in controlling bud morphology during replication stress.

The aforementioned results indicate that a pathway requiring Rad53 may control Cdk1 activity during S phase, when most bud growth takes place. Because different checkpoint mutants undergo HU-induced, Swe1-dependent elongated bud growth, we analyzed lysates of HU-treated cells by Western blotting using Swe1 antibodies (Fig. 4 A). Treatment of wild-type cells with HU for 1 or 2 h resulted in accumulation of moderately phosphorylated Swe1, which then became hyperphosphorylated after 3 h, ultimately resulting in its destruction (4 h), which is consistent with the results of Fig. 1 A of Liu and Wang (Liu and Wang, 2006). In contrast, in HU-treated *rad53Δ* mutants, only moderately phosphorylated species of Swe1 accumulated, and Swe1 largely failed to get degraded (Fig. 4 A); this was not caused by cell cycle effects, as the budding index of *rad53Δ* mutants was similar to that of wild-type cells and cells did not reenter the cell cycle (Fig. S3 A, available at http://www/jcb.org/cgi/content/full/jcb.200605080/DC1). Importantly, this

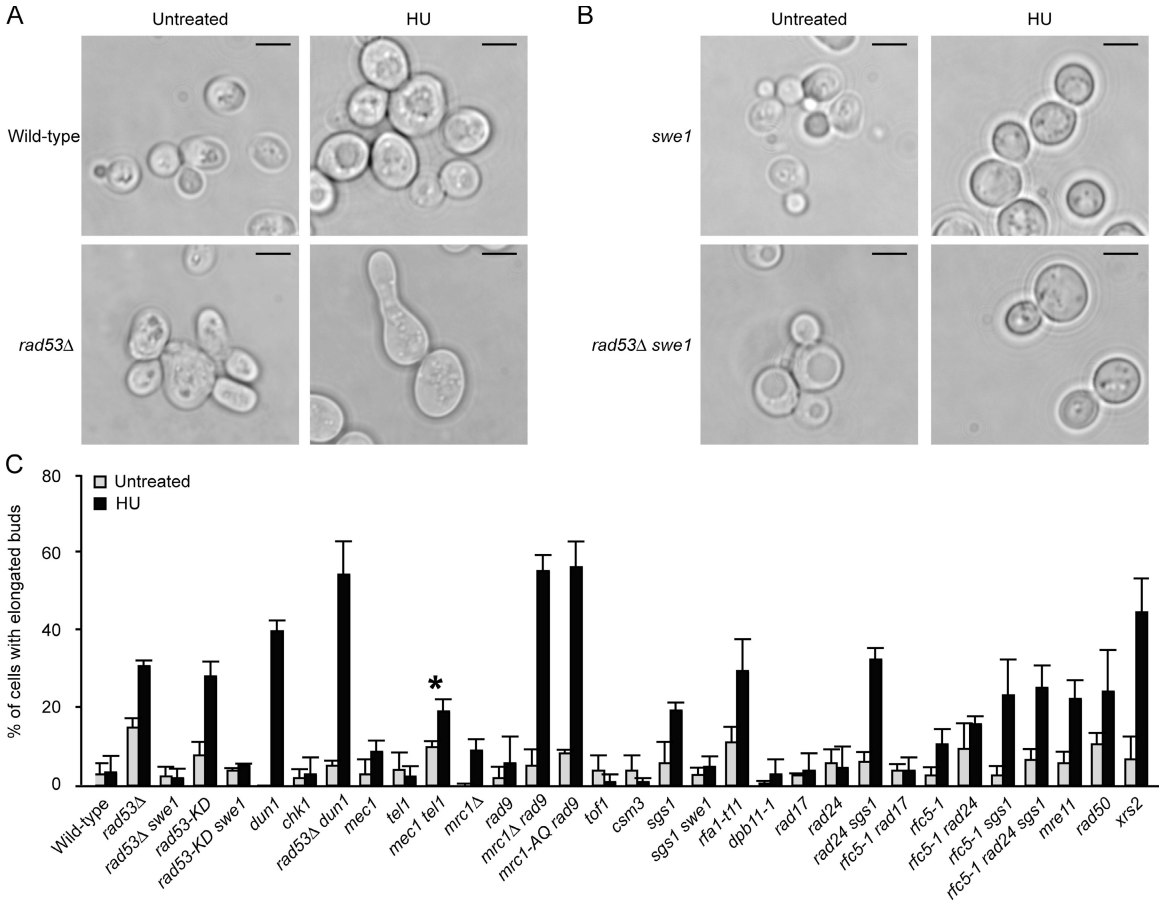

Figure 3. **Swe1-dependent regulation of bud morphology by checkpoint mutants during DNA replication stress.** (A) Prolonged DNA replication stress induces formation of elongated buds in *rad53Δ* mutants. Differential interference contrast images were taken of cultures treated with 200 mM HU for 16 h. (B) Deletion of *SWE1* rescues HU-induced elongated bud growth. Cells were treated and imaged as in A. (C) Quantification of HU-induced elongated bud growth in replication checkpoint mutants. Strains were treated with 200 mM HU for 16 h, after which the fraction of cells with elongated buds was determined out of the total population of large-budded cells. *mec1 tel1* mutants have a severe growth defect and often lyse upon HU treatment; therefore, this number (asterisk) is likely to be an underestimate. S288c strains were used. Error bars represent the SD. Bars, 5 μm.

resulted in hyperphosphorylation of Y19 of Cdk1 (Fig. 4 B), which, as expected, was Swe1-dependent (unpublished data). A similar effect of a *rad53Δ* mutation was seen with W303 *RAD5* and W303 *RAD5 rad53Δ sml1* strains (unpublished data). When analyzed as a control, Y19 of Cdk1 also became hyperphosphorylated in *hsl1* and *elm1* mutants, which are known to be defective in degradation of Swe1 (Fig. S3 B). Furthermore, high levels of Swe1 accumulated in *rad9 mrc1Δ* mutants (Fig. 4 A), which is consistent with the fact that Rad9 and Mrc1 are upstream regulators of Rad53. Swe1 levels were also elevated in *cla4* mutants (Fig. 4 A), which is consistent with the known role of Cla4 in phosphorylating Swe1 to target it for destruction.

For Swe1 to be hyperphosphorylated it needs to localize to the bud neck (Lee et al., 2005), which is dependent on various factors, including septins. We could not detect endogenous GFP-tagged Swe1 (unpublished data), but, when overexpressed, we could detect bud neck–localized Swe1-GFP in 50–60% of the cells (Fig. 4 C), in accordance with a previous study (Asano et al., 2005). Importantly, we found that Swe1 localization in *rad53Δ* mutants was similar to that of wild-type cells, even after treatment with HU (unpublished data), showing that the defect in Swe1 degradation does not result from failure to localize Swe1 to the bud neck. Altogether, these data show that a Rad53-dependent pathway restricts bud growth when cells are confronted with DNA replication stress by controlling Swe1-Cdk1.

Additional pathways control the actin cytoskeleton and bud morphogenesis during replication stress

Various pathways are known to control the actin cytoskeleton and bud morphogenesis (Pruyne and Bretscher, 2000a,b). Because we found that checkpoint proteins control bud morphology during replication stress, one would predict that defects in known pathways that regulate bud morphology might also result in HU-induced elongated bud growth. Based on knowledge from the literature (Pruyne and Bretscher, 2000a,b), we tested several candidates in an attempt to identify the pathways that may be used by the replication stress checkpoints to ensure proper bud growth during replication stress. The results of this analysis, described in this section, show that regulation of bud morphology is an essential part of the response to DNA replication stress, and that cells use a network of diverse pathways to ensure proper bud morphology when confronted with replication stress.

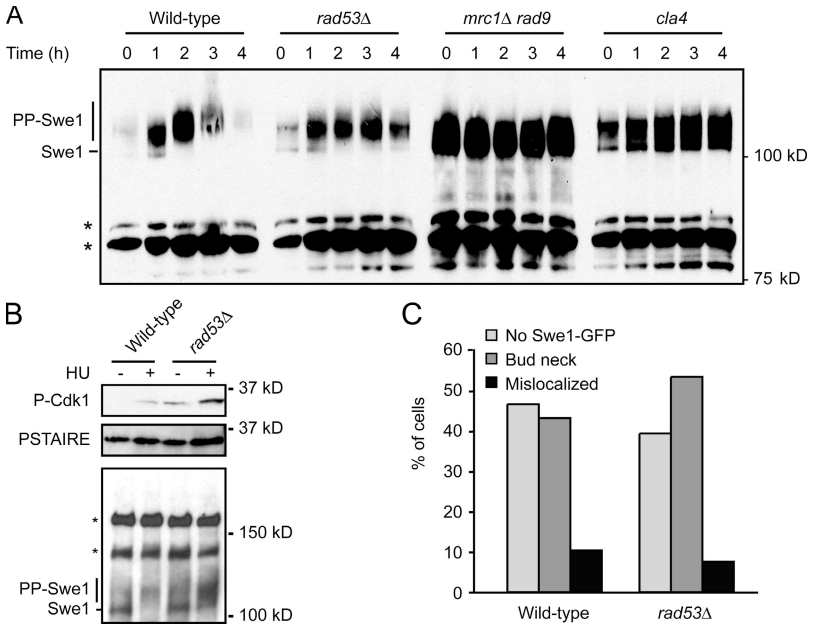

Figure 4. **Regulation of Swe1 by DNA replication checkpoint proteins.** (A) Checkpoint mutants fail to degrade Swe1 upon prolonged replication stress. Cells were treated with 200 mM HU for the indicated times, and lysates were analyzed on Western blot for Swe1. Swe1 appears as a smear caused by multiple phosphorylations (PP-Swe1). Asterisks represent proteins that cross-react with the Swe1 antibody. (B) Increased phosphorylation of Cdk1 on Y19 in *rad53Δ* mutants. Cells were left untreated or treated with 200 mM HU for 4 h, and lysates were analyzed for phosphorylation of Y19-Cdk1 on Western blot using phospho-specific Cdk1 antibodies (top) and PSTAIRE antibodies for a loading control (middle). Swe1 levels were examined on Western blot using Swe1 antibodies (bottom). Asterisks represent proteins that cross-react with the Swe1 antibody. (C) Swe1 localization is normal in *rad53Δ* mutants. Budded cells from log-phase cultures expressing Swe1-GFP were analyzed for Swe1 localization by fluorescence microscopy. S288c strains were used.

The p21-activated kinase–like kinase Cla4 is a key factor in regulation of the actin cytoskeleton, and is a central component of the Cdc42 pathway. We not only found that the Cdc24–Cdc42 pathway may not be properly down-regulated in several checkpoint mutants after HU treatment (Fig. 2 D) but also that *cla4* mutants accumulate Swe1 during replication stress (Fig. 4 A). Therefore, we tested whether *cla4* mutants might be defective in HU-induced actin depolarization. Indeed, *cla4* mutants failed to depolarize the actin cytoskeleton and dramatically elongated their buds upon HU treatment (Fig. 5 A; quantified in Fig. 5, B and C), indicating that Cla4 is necessary for regulation of the actin cytoskeleton when cells are confronted with replication stress. Interestingly, *CLA4* also genetically interacts with *RAD53* (see below). Bem1 is another component of the Cdc24–Cdc42 pathway. We found that *bem1* mutants, like *cla4* mutants, failed to depolarize actin upon HU treatment, resulting in elongated bud growth. We also tested strains lacking GTPase-activating proteins for the small Ras-like GTPases Cdc42 and Rho, which function in septin organization and bud growth (Caviston et al., 2003). Cells lacking the Bem2 and Bem3 failed to depolarize the actin cytoskeleton and elongated their buds after HU treatment, whereas *lrg1* and *rgd1* mutants responded to HU like wild-type cells (Fig. 5, B and C). This supports our finding that proper regulation of the Cdc42–Cla4 pathway is important for control of the actin cytoskeleton and cell morphology in response to HU. These results also suggest a possible involvement of specific *bem2*-controlled Rho pathways.

The kinases Elm1 and Gin4 function in septin ring assembly (Bouquin et al., 2000). The septin ring itself serves as a scaffold to bind various proteins, including Hsl1, Gin4, Elm1, and Hsl7. Hsl7 is an adaptor protein that helps recruit Swe1, bringing it into proximity of several kinases, including Hsl1, Clb2-Cdk1, Cla4, and Cdc5, which phosphorylate Swe1 to target it for degradation (Asano et al., 2005). Consistent with a role of Swe1 in regulating bud growth in response to HU, *hsl1*, *hsl7*, *gin4*, and *elm1* mutants failed to depolarize their actin cytoskeleton and formed hyperpolarized buds after treatment with HU (Fig. 5, B and C, and not depicted).

We also found that cells lacking a variety of cell cycle regulators, such as the transcription factors Swi4, Swi6, and Fkh2, the F-box protein Grr1 (Fig. 5 C and not depicted), and the mitotic exit–regulating proteins Kel2 and Dbf2, hyperpolarized bud growth upon HU treatment. Swi4 and Swi6 are involved in transcriptional control of various genes, including Hsl1, Kcc4, and Gin4 (Spellman et al., 1998; Iyer et al., 2001; Flick and Wittenberg, 2005), which might explain why *swi4* and *swi6* mutants elongate their buds upon HU treatment. It is not clear why *fkh2* mutants elongate their buds after treatment with HU, but it was previously found that a *cla4* deletion synthetically interacts with *fkh2*, indicating a role for Fkh2 in the Cdc42–Cla4 pathway (Goehring et al., 2003). Kel2, Dbf2, and Grr1 regulate mitotic exit and actomyosin ring contraction. We are currently investigating why HU induces elongated bud growth in cells lacking these factors.

Bni1 is a member of the polarisome and functions together with Cla4 in septin organization. *bni1* mutants did not develop elongated buds when challenged with HU, but instead appeared to undergo an extra round of cell growth, resulting in formation of ”strings” of cells (graphically displayed in Fig. 5 D and quantified in Fig. 5 E). We also noticed that *dbf2*, *swi4*, and *swi6* mutants form such strings of cells, whereas deletion of any of the Rho–GTPase-activating proteins or the septin-regulating kinases tested in our study had no such effect. Thus, Bni1, Dbf2, Swi4, and Swi6 also appear to assure that cells maintain proper morphology when challenged with prolonged replication stress.

Rad53 is involved in cytokinesis and shows genetic interactions with the septin pathway

If regulation of actin, septins, and cell morphology is part of the response to replication stress, one would predict that cells

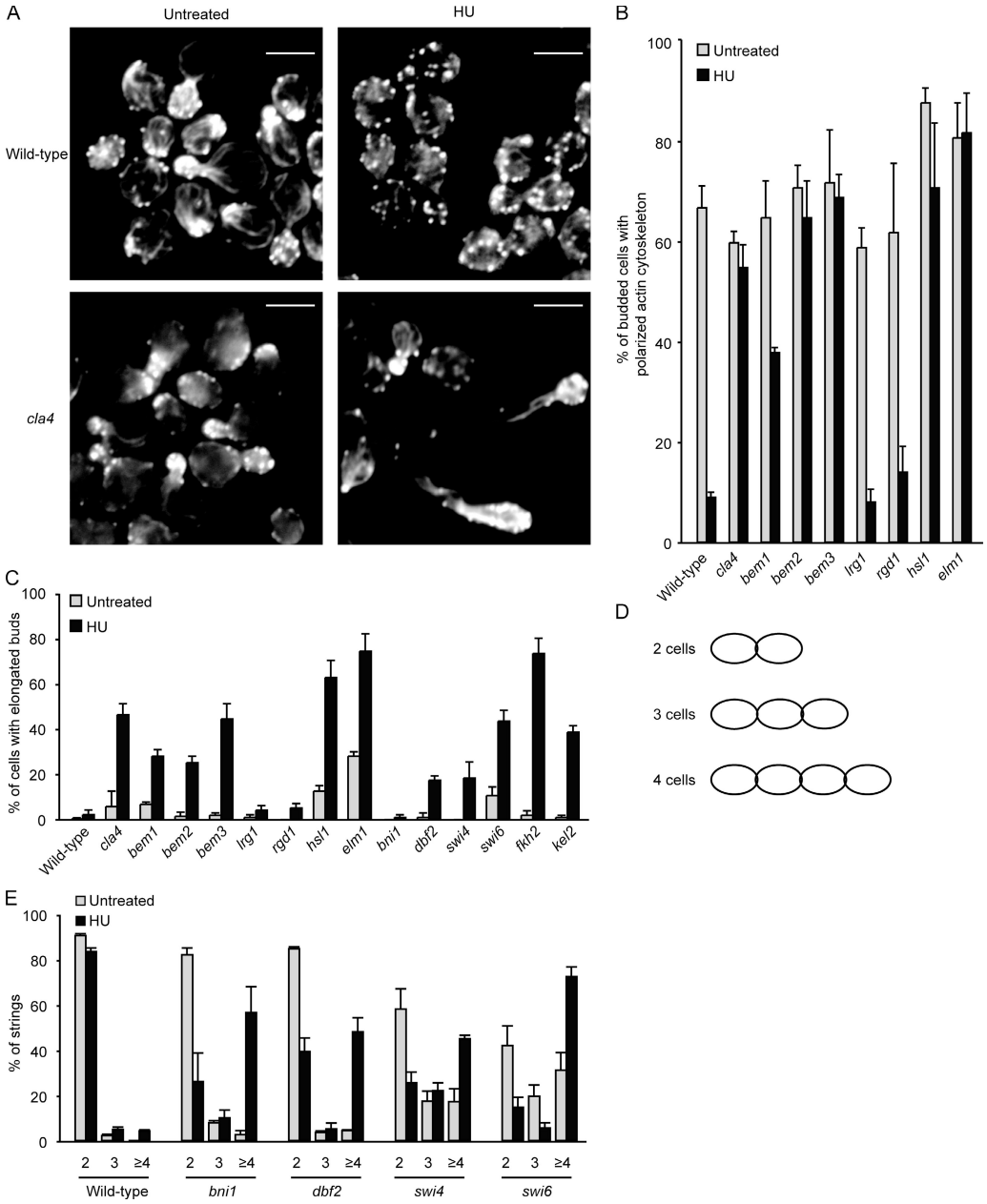

Figure 5. **Additional pathways participate in regulation of the actin cytoskeleton and bud morphology during DNA replication stress.** (A) Cla4 is essential for HU-induced actin cytoskeleton depolarization. Wild-type cells or *cla4* mutants were treated with 200 mM HU for 4 h, fixed, and stained for F-actin using rhodamine-phalloidin. Bar, 5 μm. (B) Quantification of HU-induced actin depolarization in various strains. Strains (all BY4741 background) lacking components of Rho (*lrg1*, *rgd1*, and *bem2*), Cdc42 pathways (*cla4*, *bem1*, and *bem3*), and septin-localized kinases (*hsl1* and *elm1*) were treated and processed as in A, and at least 100 budded cells per strain were counted to determine the fraction of cells with a polarized actin cytoskeleton. (C) Quantification of HU-induced elongated bud growth in replication checkpoint mutants. Strains were treated with 200 mM HU for 16 h, after which the fraction of cells with elongated buds was determined out of the total population of large-budded cells. (D) Graphic representation of strings of cells. (E) HU induces formation of strings of cells in *bni1*, *dbf2*, *swi4*, and *swi6* mutants. Cells were treated with HU for 16 h, after which strings of cells consisting of two, three, or four or more cells were counted. The fraction of strings consisting of the indicated number of cells was determined out of the total number of strings. Unbudded cells were disregarded. Error bars represent the SD. BY4741 strains were used.

defective in these pathways are more sensitive to HU. Indeed, chronic treatment of strains lacking Cla4, Elm1, Hsl1, Hsl7, and Gin4 with HU caused reduced growth compared with wild-type cells (Fig. 6 A). Analysis of the colonies that formed on HU plates showed that these mutants formed elongated buds and clusters of cells with multiple unseparated cell bodies (unpublished data), indicating that cell proliferation may have slowed because of morphological aberrations rather than an inability to activate the replication checkpoint. All of these mutants, including *cla4*, recovered normally from a 4-h HU arrest, indicating that all mutants are checkpoint proficient, whereas additional deletion of *RAD53* in these mutants resulted in a complete loss of viability (Fig. S4 A, available at http://www.jcb.org/cgi/content/full/jcb.200605080/DC1). *swe1* mutants also recovered

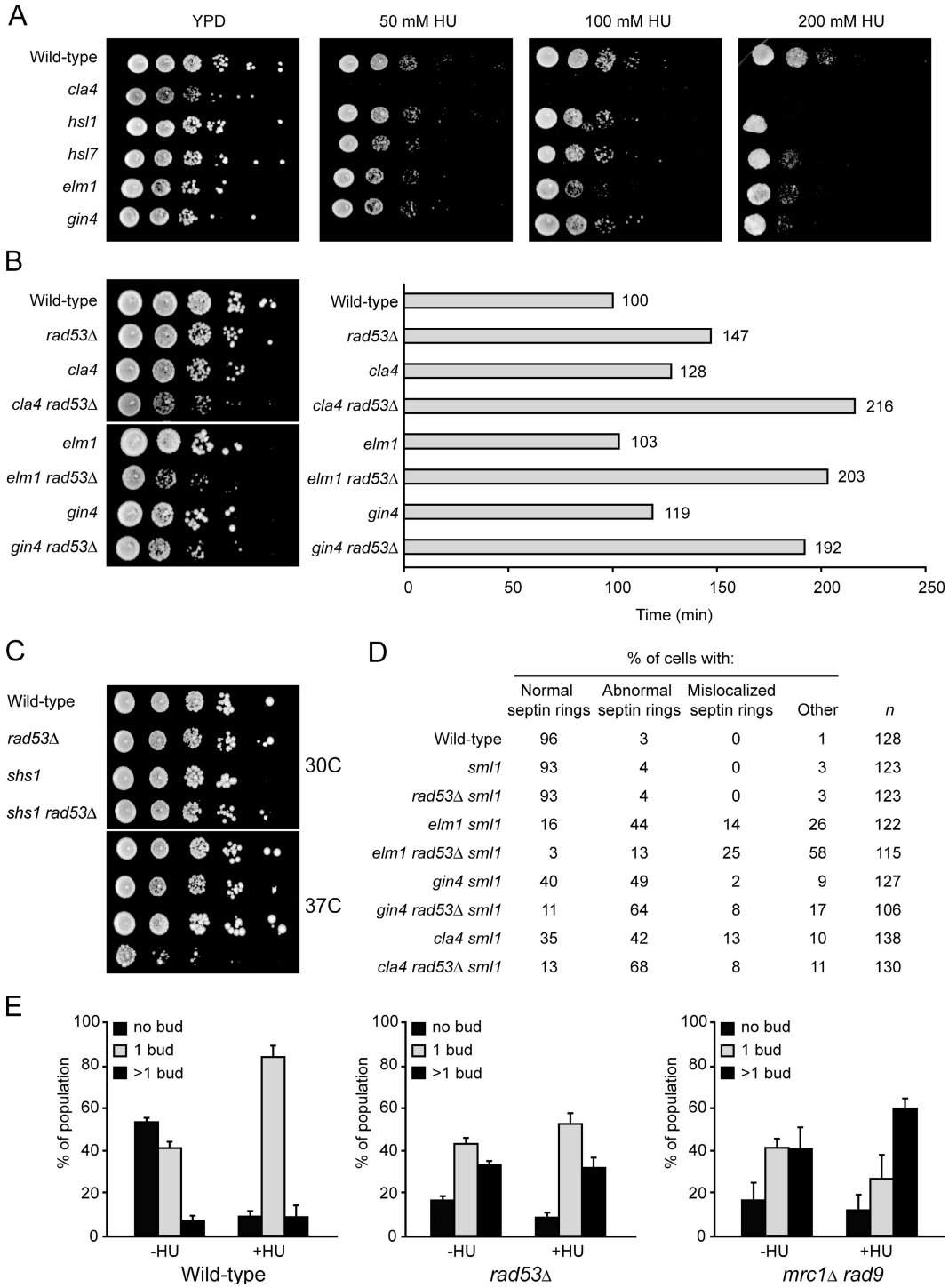

Figure 6. **Rad53 has a redundant function in septin ring organization.** (A) Mutants defective in regulation of septins and Swe1 are sensitive to HU. 10-fold dilutions of cultures were spotted on either YPD or on 200 mM HU. (B) Genetic interaction between *RAD53* and regulators of septins. (left) 10-fold dilutions of cells were spotted on YPD plates and grown at 30°C. (right) Doubling times of the indicated strains in liquid YPD. (C) Genetic interaction between *RAD53* and *SHS1*. 10-fold dilutions of cells were spotted on YPD plates and grown at the indicated temperatures. (D) Rad53 functions in septin organization. Cells were fixed and stained with anti-Cdc11 antibodies, and the percentage of cells with the indicated septin phenotypes was determined. (E) Replication checkpoint mutants have a cytokinesis defect. Cells were left untreated or treated with HU for 4 h. Subsequently, cells were treated with zymolase (5 mg/ml in 1 M sorbitol to prevent cell lysis for 30 min at 30°C) and the numbers of cells with no bud, one bud, or two or more buds were determined. Error bars represent the SD. S288c strains were used.

normally from HU arrest, whereas the *swe1 rad53Δ* double mutant did not recover, indicating that our finding that a *swe1Δ* mutation suppresses some of the morphological defects of a *rad53Δ* mutant is unrelated to an effect on checkpoint regulation of cell cycle arrest. These results suggest that septin/Swe1-regulating factors are unlikely to be directly involved in

checkpoint control of cell cycle arrest, but instead have a different function in the cellular response to replication stress, such as ensuring proper bud growth.

CLA4 has been found to genetically interact with a variety of DNA replication, repair, and checkpoint factors (Fig. S4 B; Goehring et al., 2003; Pan et al., 2006). In line with this, we found that a *rad53Δ* mutation caused synthetic fitness defects when combined with mutations in *CLA4*, *ELM1*, and *GIN4* (Fig. 6 B) and caused temperature-sensitive growth when combined with a mutation in *SHS1* (Fig. 6 C). These results indicate that Rad53 may cooperate with the pathway involving Cla4, Elm1, Gin4, and Shs1. Therefore, we tested whether Rad53 is involved in septin organization. We studied septin ring organization by immunofluorescence rather than expression of Cdc12-GFP because we found that Cdc12-GFP weakly interfered with septin organization (unpublished data). Interestingly, whereas *rad53Δ* mutants had no noticeable septin defect, deletion of *RAD53* augmented the septin defects of *elm1*, *gin4*, and *cla4* mutants (Fig. 6 D; see Fig. S4 C for examples of septin phenotypes). These data indicate that Rad53 has a redundant function in the organization of septin rings.

Finally, we observed that a *rad53Δ* deletion, as well as mutations in upstream regulators of Rad53, often lead to formation of small aggregates of cells (Fig. 1 A), indicating that Rad53 may also be involved in regulation of cytokinesis. Therefore, we treated cells with zymolase to digest the cell wall, which results in removal of the buds of cells that have successfully completed cytokinesis, but preserves the buds of cells that have not completed cytokinesis, as these cells contain buds that are still connected through the plasma membrane. We found that log-phase cultures of wild-type cells contained ∼40% of cells with a single bud and 7% of cells with more than one bud after zymolase treatment (Fig. 6 E). In contrast, zymolase treatment of *rad53Δ* mutants, as well as *mrc1Δ rad9* mutants, left 36 and 41% of cells with two or more buds, respectively, indicating that these cells failed to complete cytokinesis (Fig. 6 E). Treatment of cells with HU modestly increased the number of multibudded cells in *mrc1Δ rad9* mutants and did not increase the number of multibudded cells in wild-type and *rad53Δ* cultures. In addition, *rad53-KD* mutants also had cytokinesis defects (unpublished data). Based on these results, we conclude that Rad53 kinase activity is required for the successful completion of cytokinesis and separation of mother and daughter cells.

Discussion

During replication stress, cells of most wild-type *S. cerevisiae* strains (see second to last paragraph of this section) arrest with spherically shaped buds approximately the same size as the mother cell, indicating that mechanisms exist to monitor and control cell growth and morphology when DNA replication has halted. We observed that checkpoint mutants were frequently misshapen, had defective cell walls, and displayed hyperphosphorylation of Slt2. This is in line with a recent report showing genetic interactions between Rad9 and Slt2 (Queralt and Igual, 2005). Checkpoint proteins were also found to support proper bud site selection, indicating an involvement in maintenance of cell polarity and control of the actin cytoskeleton (Pruyne and Bretscher, 2000a,b). Indeed, we found that checkpoint proteins, including Rad53, are involved in the removal of Cdc24 and Sec4 from the bud tip during replication stress, resulting in depolarization of the actin cytoskeleton, and that failure to do so resulted in the formation of elongated buds. We identified several additional pathways involved in preventing elongated bud growth during replication stress, and at least some of these pathways (e.g., the Cla4 pathway) genetically interact with the Rad53 pathway. Our results indicate that checkpoints and additional pathways cooperate to support cell morphology and cytokinesis during chronic replication stress.

To identify the checkpoint pathways that restrict bud growth during replication stress, we tested mutants lacking a wide range of checkpoint factors. Mutations in *SGS1* and *RFA1*, but not in other genes (i.e., *RAD24, RFC5*, or *DBP11*) thought to encode upstream-acting checkpoint factors, caused a significant defect in control of cell morphology during replication stress (Fig. 3 C). Although a *rad24* single mutant had no defects, *sgs1 rad24* double mutants had a more severe phenotype than *sgs1* single mutants, in line with previous reports showing that *sgs1 rad24* double mutants have increased sensitivity to HU and methylmethanesulfonate (Frei and Gasser, 2000). Consistent with this, Rad53 and its downstream-acting factor Dun1 were involved in controlling cell morphology during replication stress. Mec1 is generally thought to function upstream of Rad53 in checkpoint signaling. Although *mec1* and *tel1* single mutants did not have a strong morphological phenotype, *mec1 tel1* double mutants had morphological aberrations that were comparable to those of *rad53Δ* and *rad53-KD* mutants. This fits with the view that Mec1 and Tel1 can have redundant functions, and is reminiscent of the Mre11 complex–mediated S phase checkpoint response that is Tel1-dependent, but is predominantly seen in the absence of Mec1 (Usui et al., 2001). Indeed, we found that the MRX complex is important for maintaining proper morphology in response to HU treatment. In addition, we found that Mrc1 and Rad9 together were required for the morphological response to replication stress, which is consistent with the finding that these proteins are redundant activators of Rad53 (Alcasabas et al., 2001). Defects in Chk1 did not cause morphological defects, which is not surprising because *chk1* mutations do not cause sensitivity to HU (Sanchez et al., 1999). Finally, mutations in *TOF1* and *CSM3* did not cause morphology defects, suggesting that there is redundancy among these genes or that they act in different aspects of checkpoint responses. Overall, the results presented in this study link replication stress checkpoint functions to the control of cell morphology.

A recent study has shown that *mec1* and *rad53Δ* mutants show premature spindle elongation during HU-induced replication stress because of failure to inhibit the microtubule-associated proteins Cin8 and Stu2, resulting in precocious chromosome segregation (Krishnan et al., 2004). This raises the possibility that the defects in regulation of morphology and spindle dynamics in checkpoint mutants may be related. Premature spindle elongation is not sufficient for HU-induced bud elongation in checkpoint mutants because *mec1* mutants, which elongate their spindles prematurely (Krishnan et al., 2004), do not show

HU-induced elongated bud growth. Furthermore, nocodazole treatment, which inhibits spindle elongation, did not block HU-induced elongated bud growth in *rad53Δ* mutants (Fig. S4 D), indicating that premature spindle elongation is not required for elongated bud growth induced by HU treatment of checkpoint mutants.

In contrast to *S. pombe* and higher eukaryotes, *S. cerevisiae* does not target Cdk1 to block cell cycle progression during replication stress, but instead directly targets processes such as late origin firing and chromosome segregation (Santocanale and Diffley, 1998; Sanchez et al., 1999). Rather, *S. cerevisiae* Cdk1 has taken on a different role; it is essential for the morphogenetic switch from polar to isotropic bud growth, and mutants that fail to degrade Swe1 have a delayed morphogenetic switch, resulting in elongated bud growth. We found that a Rad53-dependent pathway is important for timely degradation of Swe1 during replication stress, and showed genetically that it is this failure of checkpoint mutants to degrade Swe1 that results in elongated bud growth. However, it is currently unknown how Rad53 controls Swe1. Swe1 recruitment to septin rings was unaffected in *rad53Δ* mutants, which is consistent with our finding that septin organization is normal in these mutants. In *S. pombe*, the Rad53 homologue Cds1 may directly phosphorylate Wee1 to control its activity (Boddy et al., 1998), raising the possibility that in *S. cerevisiae* Rad53 also directly phosphorylates Swe1. However, it is also possible that Rad53 indirectly controls Swe1 levels. For instance, Rad53 may target kinases that in turn directly phosphorylate Swe1, like Cdc5 and Cla4 (Lee et al., 2005). Indeed, Rad53 has been suggested to control Cdc5 activity (Sanchez et al., 1999).

We found that *RAD53* genetically interacts with a variety of upstream regulators of septins, as well as with the nonessential septin *SHS1*. Furthermore, replication stress checkpoint mutants showed a cytokinesis defect, which is often linked to septin malfunction. Therefore, we investigated the possibility that Rad53 may affect septin organization. We found that Rad53 by itself is not essential for the organization of septin rings, but has a redundant role with upstream septin regulators like Cla4, Gin4, and Elm1 in septin organization and cell growth. Consistent with this, defects in septin-regulating factors caused sensitivity to HU and HU-induced bud elongation. Although the molecular nature of the Rad53 interactions with septins is not yet clear, interestingly, Rad53 can directly phosphorylate Shs1 in vitro, and a pool of Rad53 may localize to the septin ring in vivo (see Smolka et al. on p. 743 of this issue). It is possible that defects in this cooperation could explain the deregulation of Swe1 that occurs in checkpoint mutants in response to HU. Further studies are needed to unravel the function of Rad53 in control of septin organization.

Bud morphogenesis during replication stress has been studied previously. Several studies have shown that replication stress induced filamentous differentiation strongly in one wild-type strain (Σ1278b), weakly in two wild-type strains (W303 *rad5-535* and A374), and not at all in another wild-type strain (S288c; Jiang and Kang, 2003; Liu and Wang, 2006). Induction of this phenotype in Σ1278b cells appeared to require Mec1, Rad53, and Swe1, but not Sgs1 or Dun1. The HU-induced bud elongation phenotype we have studied does not occur in our wild-type strain (S288c) and is induced in various checkpoint mutants, and thus appears to be a different phenotype. To better understand the differences between wild-type strains, we tested seven different laboratory wild-type strains collected over the years and identified one strain showing a strong bud elongation phenotype (DBY745), two strains showing a weaker phenotype (W303 *RAD5* and W303 *rad5-535*), and five strains (MGD, BY4741, L2955, Y55, and JKM139) that did not show HU-induced bud elongation. Because DBY745 was derived by crossing markers into S288c (unpublished data, Botstein, D., personal communication) and JKM139 was derived by crossing markers from Y55 into DBY745 (unpublished data, Haber, J., personal communication), it seems likely that the bud elongation resulted from a mutation introduced during the construction of DBY745. Similarly, the bud elongation phenotype of the W303 strains may have resulted from the introduction of a mutation during the intercrossing of the S288c derivatives used to construct W303 (for detailed information on W303 see the *Saccharomyces* Genome Database; www.yeastgenome.org). Further analysis will be required to understand the exact genetic basis for the replication stress–induced bud elongation and filamentous differentiation that some wild-type strains show.

In conclusion, we found that replication stress checkpoint proteins like Rad53 function together with additional pathways to promote the timely degradation of Swe1, thereby relieving inhibition of Cdk1. Cdk1 then induces the switch from polar to isotropic bud growth, thus preventing elongated bud growth and contributing to cell viability because such elongated buds are susceptible to cell wall stress. Therefore, replication stress checkpoint–mediated control of bud morphology is part of the response to replication stress and contributes to cell survival.

Materials and methods

Strains, plasmids, and growth conditions

S. cerevisiae strains were grown in standard YPD medium or synthetic complete medium lacking the appropriate amino acid. Strains were directly derived from the S288c strain RDKY3615 using either standard gene replacement methods or intercrossing (Table S1, available at http://www.jcb.org/cgi/content/full/jcb.200605080/DC1). To construct cells harboring the *mrc1-AQ* allele, a *TRP1* cassette was inserted into a PacI site 250 bp downstream of the *mrc1-AQ* allele in plasmid pAO138 (gift from S. Elledge, Harvard Medical School, Boston, MA). Subsequently, *mrc1-AQ.TRP1* was PCR amplified and used to replace a *URA3* cassette previously inserted at the *MRC1* locus. All other strains were obtained from the systematic deletion project (BY4741; derived from the same parental strains as RDKY3615, i.e., S288c) and were only used when specifically stated in the figure legends. Plasmids pRS414-*ADH-CDC24-GFP* and pRS415-*ADH-CDC24-GFP* were provided by M. Peter (Swiss Federal Institute of Technology, Zurich, Switzerland), and pRS414-*GFP-SEC4* was obtained from S. Emr (University of California, San Diego, La Jolla, CA). The YepT-*SWE1-GFP* plasmid was obtained from K. Lee (National Institutes of Health, Bethesda, MD).

Microscopy

Live cells (expressing either Cdc24-GFP, Sec4-GFP, or Swe1-GFP) were imaged at room temperature in synthetic complete medium with an inverted microscope (Eclipse TE300; Nikon) equipped with a 100×/1.40 NA Plan Apo objective lens (Nikon), using a charge-coupled device camera (Orca-ER; Hamamatsu) and MetaMorph software (Universal Imaging Corp.), and images were processed using Photoshop and Illustrator software (both Adobe). Alternatively, cells were fixed with 3.7% formaldehyde and either stained with 50 μg/ml Calcofluor white or rhodamine-phalloidin according

to manufacturer's instructions (Invitrogen) or processed for septin immunofluorescence, as previously described (Pringle, 1991). Rabbit anti-Cdc11p antibodies (Santa Cruz Biotechnology, Inc.) were used at 1:10 dilution, followed by TRITC–conjugated goat anti–rabbit secondary antibody at a 1:50 dilution (Jackson ImmunoResearch Laboratories). Fixed cells were embedded in Vectashield HardSet mounting medium (Vector Laboratories) to reduce photobleaching. At least 100 cells were counted per strain and per treatment. For analysis of bud scar positioning, only cells with at least three bud scars were counted. Scars were scored as "normal" when all scars on a cell were located at the same pole. When one or more scars deviated from that pole, bud scar positioning was scored as "abnormal."

Cell extracts and Western blot analysis

Log-phase cells were treated with HU as indicated, pelleted, and resuspended in hot (95°C) Laemmli sample buffer supplemented with protease inhibitors and boiled for 5 min, after which glass beads were added and cells were vortexed for 15 min at 4°C. After centrifugation, soluble proteins were analyzed by SDS-PAGE and Western blot using phospho-Cdc2 antibodies (New England Biolabs) to analyze Cdk1 phosphorylation. Total Cdk1 levels were determined using PSTAIRE antibodies (Millipore). Antibodies against Swe1 were provided by D. Kellogg (University of California, Santa Cruz, Santa Cruz, CA). Phosphorylated Slt2 was analyzed with phospho-specific p42/44 MAPK antibodies (Cell Signaling Technology), and pan-Slt2 was detected using Slt2 antibodies (Santa Cruz Biotechnology, Inc.). Detection was performed using the SuperSignal West Femto Detection kit according to the manufacturer's instructions (Pierce Chemical Co.).

Zymolase sensitivity

10 ml of cells were grown to OD_{600} of 1 and quickly washed with 15 ml H_2O. Cells were then resuspended in 10 ml hypotonic buffer (10 mM Hepes, pH 7.5) supplemented with 20 U/ml lytic enzyme (Puregene) and incubated at 30°C with occasional agitation. OD_{600} was measured every 15 min.

Bud elongation

100 µl of 1–2 M HU in H_2O was added to 1 ml log-phase cells (in YPD), followed by 8–16 h at 30°C while shaking. The fraction of cells with elongated buds was determined as the percentage of large-budded cells only (unbudded and small-budded cells were ignored). A bud was scored as "elongated" when the length of the bud was at least twice its width.

Cytokinesis assay

1 ml of log-phase cells was washed with PBS and incubated at 30°C in 25 mM Hepes, pH 7.5, containing 1 M sorbitol (for osmotic support), and 5 mg/ml zymolase. After 30 min, cells with no buds, one bud, or two or more buds were counted. At least 100 cells were counted per treatment.

Halo assay

Halo assays were performed as previously described (Ayscough et al., 1997). In brief, 250 µl of a log-phase YPD culture was diluted in 3.5 ml YPD, after which 3.5 ml molten Agarose (1% wt/vol) in YPD (cooled to ~50°C) was added. The cell suspension was then poured onto a YPD plate. Paper disks (6 mm diam; Becton Dickinson) were placed on top of the plates, and either 10 µl latrunculin A or 10 µl DMSO were spotted onto the center of the disks. Plates were inverted and incubated at 30°C until halos were visible.

Determination of doubling times

Overnight cultures (prestationary phase) were diluted in 50 ml fresh, prewarmed YPD to an OD_{600} of 0.05. Cells were then incubated at 30°C while shaking. 1-ml samples were taken every hour for 12 h, and doubling times were determined using Excel (Microsoft).

Online supplemental material

Table S1 shows S288c-derived strains used in the described studies. Fig. S1 shows analysis of the sensitivity of various S phase checkpoint mutants to Calcofluor white, images of the actin cytoskeleton in *mec1*, *tel1*, *sgs1*, and *chk1* mutants upon treatment with HU, and the failure of *rad53Δ* mutants to remove Sec4 from the bud tip during replication stress. Fig. S2 shows analysis of metabolic activity of HU-treated wild-type and *rad53Δ* mutants during prolonged replication stress, images of *SWE1*-dependent HU-induced bud elongation in *rad53-KD* and *sgs1* cells. Fig. S3 shows an analysis of the budding index of wild-type, *rad53Δ*, *mrc1Δ rad9*, and *cla4* mutants that shows that none of these mutants reenter the cell cycle during HU arrest, and a Western blot demonstrating hyperphosphorylation of Y19 of Cdk1 during HU arrest in *elm1* and *hsl1* mutants. Fig. S4 shows that upstream regulators of septins are replication checkpoint proficient, extensive genetic interactions between *CLA4* and DNA replication, repair, checkpoint genes, examples of various septin phenotypes, and that HU-induced bud elongation in *rad53Δ* mutants is not blocked by nocodazole. Online supplemental material is available at http://www.jcb.org/cgi/content/full/jcb.200605080/DC1.

We thank members of the Kolodner laboratory, D. Kellogg, and Matt Gentry for insightful discussions and helpful suggestions, Ellen Kats for construction of strains, and Hilde Abrahamsen and Kristina Schmidt for critical reading of the manuscript.

This work was supported by National Institutes of Health grants GM26017 (R.D. Kolodner) and HG002604 (H. Zhou). J.M. Enserink is a recipient of a fellowship from the Dutch Cancer Society (Koningin Wilhelmina Fonds/Kankerbestrijding).

The authors have no commercial affiliations or conflicts of interest.

Submitted: 17 May 2006
Accepted: 30 October 2006

References

Alcasabas, A.A., A.J. Osborn, J. Bachant, F. Hu, P.J. Werler, K. Bousset, K. Furuya, J.F. Diffley, A.M. Carr, and S.J. Elledge. 2001. Mrc1 transduces signals of DNA replication stress to activate Rad53. *Nat. Cell Biol.* 3:958–965.

Amon, A., U. Surana, I. Muroff, and K. Nasmyth. 1992. Regulation of p34CDC28 tyrosine phosphorylation is not required for entry into mitosis in *S. cerevisiae*. *Nature*. 355:368–371.

Asano, S., J.E. Park, K. Sakchaisri, L.R. Yu, S. Song, P. Supavilai, T.D. Veenstra, and K.S. Lee. 2005. Concerted mechanism of Swe1/Wee1 regulation by multiple kinases in budding yeast. *EMBO J.* 24:2194–2204.

Ayscough, K.R., J. Stryker, N. Pokala, M. Sanders, P. Crews, and D.G. Drubin. 1997. High rates of actin filament turnover in budding yeast and roles for actin in establishment and maintenance of cell polarity revealed using the actin inhibitor latrunculin-A. *J. Cell Biol.* 137:399–416.

Bickle, M., P.A. Delley, A. Schmidt, and M.N. Hall. 1998. Cell wall integrity modulates RHO1 activity via the exchange factor ROM2. *EMBO J.* 17:2235–2245.

Boddy, M.N., B. Furnari, O. Mondesert, and P. Russell. 1998. Replication checkpoint enforced by kinases Cds1 and Chk1. *Science*. 280:909–912.

Bouquin, N., Y. Barral, R. Courbeyrette, M. Blondel, M. Snyder, and C. Mann. 2000. Regulation of cytokinesis by the Elm1 protein kinase in *Saccharomyces cerevisiae*. *J. Cell Sci.* 113:1435–1445.

Caviston, J.P., M. Longtine, J.R. Pringle, and E. Bi. 2003. The role of Cdc42p GTPase-activating proteins in assembly of the septin ring in yeast. *Mol. Biol. Cell*. 14:4051–4066.

Cid, V.J., A. Duran, F. del Rey, M.P. Snyder, C. Nombela, and M. Sanchez. 1995. Molecular basis of cell integrity and morphogenesis in *Saccharomyces cerevisiae*. *Microbiol. Rev.* 59:345–386.

Cobb, J.A., K. Shimada, and S.M. Gasser. 2004. Redundancy, insult-specific sensors and thresholds: unlocking the S-phase checkpoint response. *Curr. Opin. Genet. Dev.* 14:292–300.

Flick, K., and C. Wittenberg. 2005. Multiple pathways for suppression of mutants affecting G1-specific transcription in *Saccharomyces cerevisiae*. *Genetics*. 169:37–49.

Frei, C., and S.M. Gasser. 2000. The yeast Sgs1p helicase acts upstream of Rad53p in the DNA replication checkpoint and colocalizes with Rad53p in S-phase-specific foci. *Genes Dev.* 14:81–96.

Goehring, A.S., D.A. Mitchell, A.H. Tong, M.E. Keniry, C. Boone, and G.F. Sprague Jr. 2003. Synthetic lethal analysis implicates Ste20p, a p21-activated potein kinase, in polarisome activation. *Mol. Biol. Cell*. 14:1501–1516.

Guo, W., D. Roth, C. Walch-Solimena, and P. Novick. 1999. The exocyst is an effector for Sec4p, targeting secretory vesicles to sites of exocytosis. *EMBO J.* 18:1071–1080.

Hartwell, L.H., and T.A. Weinert. 1989. Checkpoints: controls that ensure the order of cell cycle events. *Science*. 246:629–634.

Iyer, V.R., C.E. Horak, C.S. Scafe, D. Botstein, M. Snyder, and P.O. Brown. 2001. Genomic binding sites of the yeast cell-cycle transcription factors SBF and MBF. *Nature*. 409:533–538.

Jiang, Y.W., and C.M. Kang. 2003. Induction of *S. cerevisiae* filamentous differentiation by slowed DNA synthesis involves Mec1, Rad53 and Swe1 checkpoint proteins. *Mol. Biol. Cell*. 14:5116–5124.

Kellogg, D.R. 2003. Wee1-dependent mechanisms required for coordination of cell growth and cell division. *J. Cell Sci.* 116:4883–4890.

Kops, G.J., B.A. Weaver, and D.W. Cleveland. 2005. On the road to cancer: aneuploidy and the mitotic checkpoint. *Nat. Rev. Cancer*. 5:773–785.

Krishnan, V., S. Nirantar, K. Crasta, A.Y. Cheng, and U. Surana. 2004. DNA replication checkpoint prevents precocious chromosome segregation by regulating spindle behavior. *Mol. Cell*. 16:687–700.

Lee, K.S., S. Asano, J.E. Park, K. Sakchaisri, and R.L. Erikson. 2005. Monitoring the cell cycle by multi-kinase-dependent regulation of Swe1/Wee1 in budding yeast. *Cell Cycle*. 4:1346–1349.

Lew, D.J. 2003. The morphogenesis checkpoint: how yeast cells watch their figures. *Curr. Opin. Cell Biol.* 15:648–653.

Lisby, M., J.H. Barlow, R.C. Burgess, and R. Rothstein. 2004. Choreography of the DNA damage response: spatiotemporal relationships among checkpoint and repair proteins. *Cell*. 118:699–713.

Liu, H., and Y. Wang. 2006. The function and regulation of budding yeast Swe1 in response to interrupted DNA synthesis. *Mol. Biol. Cell*. 17:2746–2756.

Lopes, M., C. Cotta-Ramusino, A. Pellicioli, G. Liberi, P. Plevani, M. Muzi-Falconi, C.S. Newlon, and M. Foiani. 2001. The DNA replication checkpoint response stabilizes stalled replication forks. *Nature*. 412:557–561.

Lussier, M., A.M. White, J. Sheraton, T. di Paolo, J. Treadwell, S.B. Southard, C.I. Horenstein, J. Chen-Weiner, A.F. Ram, J.C. Kapteyn, et al. 1997. Large scale identification of genes involved in cell surface biosynthesis and architecture in *Saccharomyces cerevisiae*. *Genetics*. 147:435–450.

McMillan, J.N., C.L. Theesfeld, J.C. Harrison, E.S. Bardes, and D.J. Lew. 2002. Determinants of Swe1p degradation in *Saccharomyces cerevisiae*. *Mol. Biol. Cell*. 13:3560–3575.

Myung, K., A. Datta, and R.D. Kolodner. 2001. Suppression of spontaneous chromosomal rearrangements by S phase checkpoint functions in *Saccharomyces cerevisiae*. *Cell*. 104:397–408.

Osborn, A.J., and S.J. Elledge. 2003. Mrc1 is a replication fork component whose phosphorylation in response to DNA replication stress activates Rad53. *Genes Dev.* 17:1755–1767.

Ovalle, R., S.T. Lim, B. Holder, C.K. Jue, C.W. Moore, and P.N. Lipke. 1998. A spheroplast rate assay for determination of cell wall integrity in yeast. *Yeast*. 14:1159–1166.

Pan, X., P. Ye, D.S. Yuan, X. Wang, J.S. Bader, and J.D. Boeke. 2006. A DNA integrity network in the yeast *Saccharomyces cerevisiae*. *Cell*. 124:1069–1081.

Paulovich, A.G., D.P. Toczyski, and L.H. Hartwell. 1997. When checkpoints fail. *Cell*. 88:315–321.

Pringle, J.R. 1991. Staining of bud scars and other cell wall chitin with calcofluor. *Methods Enzymol.* 194:732–735.

Pruyne, D., and A. Bretscher. 2000a. Polarization of cell growth in yeast. *J. Cell Sci.* 113:571–585.

Pruyne, D., and A. Bretscher. 2000b. Polarization of cell growth in yeast. I. Establishment and maintenance of polarity states. *J. Cell Sci.* 113:365–375.

Queralt, E., and J.C. Igual. 2005. Functional connection between the Clb5 cyclin, the PKC pathway and the Swi4 transcription factor in *Saccharomyces cerevisiae*. *Genetics*. 171:1485–1498.

Sanchez, Y., J. Bachant, H. Wang, F. Hu, D. Liu, M. Tetzlaff, and S.J. Elledge. 1999. Control of the DNA damage checkpoint by chk1 and rad53 protein kinases through distinct mechanisms. *Science*. 286:1166–1171.

Santocanale, C., and J.F. Diffley. 1998. A Mec1- and Rad53-dependent checkpoint controls late-firing origins of DNA replication. *Nature*. 395:615–618.

Sorger, P.K., and A.W. Murray. 1992. S-phase feedback control in budding yeast independent of tyrosine phosphorylation of p34cdc28. *Nature*. 355:365–368.

Spellman, P.T., G. Sherlock, M.Q. Zhang, V.R. Iyer, K. Anders, M.B. Eisen, P.O. Brown, D. Botstein, and B. Futcher. 1998. Comprehensive identification of cell cycle-regulated genes of the yeast *Saccharomyces cerevisiae* by microarray hybridization. *Mol. Biol. Cell*. 9:3273–3297.

Suzuki, M., R. Igarashi, M. Sekiya, T. Utsugi, S. Morishita, M. Yukawa, and Y. Ohya. 2004. Dynactin is involved in a checkpoint to monitor cell wall synthesis in *Saccharomyces cerevisiae*. *Nat. Cell Biol.* 6:861–871.

Thornton, B.R., and D.P. Toczyski. 2003. Securin and B-cyclin/CDK are the only essential targets of the APC. *Nat. Cell Biol.* 5:1090–1094.

Usui, T., H. Ogawa, and J.H. Petrini. 2001. A DNA damage response pathway controlled by Tel1 and the Mre11 complex. *Mol. Cell*. 7:1255–1266.